Supplementary Methods

Protein Purification and *In Vitro* Transcription

Full-length LAF-1, Whi3, and GAR-1ΔN fragments were tagged with 6-His and expressed in *E. coli* using standard procedures. Cell lysis, Whi3 purification, and *BNI1* mRNA transcription were performed following Zhang et al[1]. Briefly, cells were pelleted and resuspended in lysis buffer (20 mM Tris-HCl, pH 8, 1.5 M NaCl, 20 mM Imidazole, 1 mM DTT, 1 tablet of Roche protease inhibitor cocktail, 5 uL of Benzonase nuclease). Lysate supernatant was incubated with Ni-NTA (Qiagen) in gravity columns, washed well with lysis buffer (10-column volumes), and eluted with 6-column volumes elution buffer (20 mM Tris-HCl, pH 8, 150 mM NaCl, 200 mM Imidazole, 1 mM DTT). Whi3 was stored in Whi3 elution buffer at -80^{o}C. *BNI1* DNA template was obtained using a T7 promoter TAATACGACTCACTATAGGG cloned to the 5' end of *BNI1*. Plasmids were digested using restriction enzymes in front of the T7 promoter and after *BNI1*. This DNA template was gel extracted (Qiagen), eluted in RNase-free water, and *in vitro* transcribed using HiScribe T7 high yield RNA synthesis kit (NEB) following protocols in the kit. Transcribed RNAs were ethanol-precipitated, resuspended in RNase-free water, and stored at -80^{o}C. LAF-1 and GAR-1ΔN fragment cell lysis and purification was performed following Elbaum-Garfinkle et al[2]. Cells were pelleted and resuspended in lysis buffer (20 mM Tris-HCl, pH 7.4, 500 mM NaCl, 10 mM imidazole, 14 mM Beta-mercaptoethanol (ME), 10% (vol/vol) glycerol, and 1% Triton-X, 1 mg/mL lysozyme and 1 tablet of Roche protease inhibitor cocktail). Cells were lysed by sonication and cellular debris pelleted at 20,000 g for 30 min. Lysate supernatant was incubated with Ni-NTA agarose (Qiagen) in gravity columns, washed well with Ni-Wash buffer (20 mM Tris-

HCl, pH 7.4, 500 mM NaCl, 25 mM imidazole, 14 mM Beta-ME, 10% (vol/vol) glycerol), and eluted with Ni-Elution buffer (20 mM Tris, pH 7.4, 500 mM NaCl, 250 mM imidazole, 14 mM Beta-ME, 10% (vol/vol) glycerol). Nickel purification was sufficient to purify GAR-1ΔN. For LAF-1, elution fractions were diluted 5x with room temperature Heparin binding buffer (20 mM Tris, pH 7.4, 50 mM NaCl, 1% (vol/vol) glycerol, and 2 mM DTT) and loaded onto a HiTrap Heparin column (GE). The column was washed with heparin binding buffer and eluted in 20 mM Tris, pH 7.4, 1 M NaCl, 1% (vol/vol) glycerol, and 2 mM DTT). For LAF-1 and GAR-1ΔN, glycerol was added to 10% (vol/vol) before flash freezing in liquid nitrogen and storing at -80^{o}C.

Device Design and Microfabrication

The microfluidic devices were designed using AutoCAD and have either a standard T-junction geometry with vertical and horizontal channels dimensions 20 μm x 3900 μm and 40 μm x 9400 μm, respectively (Fig. S1a) or a box geometry (Fig. S1b) with vertical and horizontal channels 20 μm x 2500 μm and box dimension 250 μm x 1000 μm. Corresponding devices were constructed using standard photolithography and soft lithography techniques. Briefly, a silicon wafer is spin coated with a 10 μm layer of SU8-2010 (Microchem), baked, covered with a photo mask described above, exposed to UV light, and developed to wash away unexposed photoresist. Following wafer silanization, polydimethylsiloxane (PDMS) and cross-linker (10:1) (Sylgard 184, Dow Corning) were poured onto the wafer, degassed under vacuum, and cured by baking at 60^{o}C for 4-6 hours. The PDMS mold was peeled off, cored for inlets and outlets (Harris Uni-Core 0.75), plasma bonded to a glass slide, and held at 60^{o}C overnight. Finally, the devices are connected to syringes (typically 250 μL or 2.5 mL) with Teflon tubing (Cole Parmer).

Device Operation

To achieve on-chip coalescence of GAR-1ΔN and LAF-1, microfluidic devices were surface treated overnight by flushing with 1 wt% pluronic at 0.01 mL/hr using a syringe pump (Chemyx). For GAR-1ΔN, devices were additionally exposed in a UVO-cleaner (Jetlight) for 7 min. Devices used with Whi3 required no surface treatment. For microrheology only experiments (Fig. S1b), a mixed solution of protein droplets and red fluorescent PEG-passivated or –COOH microspheres (Invitrogen) of 0.5 μm diameter were inserted into the top channel at 50 μL/hr and flow was stopped for image analysis. For T-junction devices (Fig. S1a), homogeneous protein solution and PEG-passivated microspheres were inserted into the main channel and flow was from left to right at 10 μL/hr. Protein droplets and PEG-passivated or –COOH microspheres were supplied via the orthogonal inlet channel and flow was from bottom to top at 50 μL/hr. Lower flow rates obtained by hydrostatic pressure for both syringes are used for image analysis. In this approach, syringes were removed from the syringe pump and fixed above the device (~ 2-3 feet).

Image Analysis for Microrheology

Microrheology analysis was performed as previously described[1–3]. Red fluorescent microspheres were encapsulated in protein phases as described above. Using a 60x oil objective on a spinning disk confocal, measurements were taken at 150-ms time intervals for 150 s. Only beads residing several micrometers away from the liquid-liquid and liquid-solid interface were included in data analysis to minimize surface effects. Mean-squared displacement (*MSD*) data were fit to the form $MSD = 4Dt^{\alpha} + NF$, where α is the diffusive exponent, D is diffusion coefficient, and NF is a constant representing the noise

floor. Here, *NF* was determined experimentally for beads stuck to a coverslip; we find $NF \approx 2\text{x}10^{-5}$ $\mu m^2/s$.

Flow Analysis

Velocity profiles are determined in both the protein-lean and protein-rich phases, discussed below. Analysis of time-lapse images of spherical probe particles is used to calculate velocity profiles. In the protein-lean phase, probe particles form streaks due to high fluid velocities and long enough exposure times. Streak length is determined by image thresholding, identification of centroids for each streak, and determination of the major axis length corresponding to each centroid. Depending on the thresholding value manually chosen, multiple centroids are sometimes found for a single streak, resulting in underestimation of the streak length (Fig. S3). This leads to points which populate lower than the actual veloctity. Velocity profiles are calculated at a given height in the device by dividing the streak length by the exposure times. In the protein-rich phase probe particles flow slower. Thus, velocities are calculated using the same particle-tracking algorithm used for microrheology.

To describe the velocity profiles in each phase at steady state, we utilize the unidirectional form of the Navier-Stokes equation for each phase

$$\frac{dP_1}{dx} = \mu_1 \left[\frac{\partial^2 v_{x,1}}{\partial y^2} + \frac{\partial^2 v_{x,1}}{\partial z^2} \right] \qquad 0 < y < w_1 \qquad -H < z < H \qquad \text{(S1)}$$

$$\frac{dP_2}{dx} = \mu_2 \left[\frac{\partial^2 v_{x,2}}{\partial y^2} + \frac{\partial^2 v_{x,2}}{\partial z^2} \right] \qquad -w_2 < y < 0 \qquad -H < z < H \qquad \text{(S2)}$$

where subscripts 1 and 2 indicate phase 1 or 2, respectively, P is dynamic pressure, μ is viscosity, x, y, and z are the spatial coordinates for fluid flow in the x direction with channel height $2H$ and $z = 0$ at the center of the channel in the z dimension, and width

$w = w_1 + w_2$ with $y = 0$ at the fluid-fluid interface. $v_{x,1}(w_1, z) = v_{x,2}(-w_2, z) = 0$ and $v_{x,1}(y, H) = v_{x,2}(y, H) = 0$ since we assume no-slip at the channel walls. $\frac{\partial v_{x,1}}{\partial z}(y, 0) = \frac{\partial v_{x,2}}{\partial z}(y, 0) = 0$ since velocity profiles are symmetric about the center of the channel in the z dimension. At the fluid-fluid interface, $v_{x,1}(0, z) = v_{x,2}(0, z)$ following the no-slip condition and $\mu_1 \frac{\partial v_{x,1}}{\partial y}(0, z) = \mu_2 \frac{\partial v_{x,2}}{\partial y}(0, z)$ following a stress balance assuming zero gradients in surface tension. Integration of Eqs. (S1) and (S2) with the boundary conditions specified gives

$$v_{x,1}(y,z) = \sum_{n=0}^{\infty} \frac{2\beta(-1)^n}{\mu_1 \lambda_n^3 H} \cos(\lambda_n z)\left[C_1 \cosh(\lambda_n y) + C_2 \sinh(\lambda_n y)\right] + \frac{\beta}{2\mu_1}\left(z^2 - H^2\right) \quad \text{(S3)}$$

$$v_{x,2}(y,z) = \sum_{n=0}^{\infty} \frac{2\beta(-1)^n}{\mu_2 \lambda_n^3 H} \cos(\lambda_n z)\left[\left(\frac{\mu_2}{\mu_1}(C_1 - 1) + 1\right)\cosh(\lambda_n y) + C_2 \sinh(\lambda_n y)\right] + \frac{\beta}{2\mu_2}\left(z^2 - H^2\right) \quad \text{(S4)}$$

where $C_2 = \dfrac{1 - \frac{\mu_2}{\mu_1} + \frac{\mu_2}{\mu_1}\frac{1}{\cosh(\lambda_n w_1)} - \frac{1}{\cosh(\lambda_n w_2)}}{\frac{\mu_2}{\mu_1}\tanh(\lambda_n w_1) + \tanh(\lambda_n w_2)}$ and $C_1 = \frac{1}{\cosh(\lambda_n w_1)} - C_2 \tanh(\lambda_n w_1)$,

$\beta = \frac{dP_1}{dx} = \frac{dP_2}{dx}$, and $\lambda_n = \frac{(2n+1)\pi}{2H}$ are eigenvalues. In the limit $\mu_1 >> \mu_2$, as is the case here, the velocity at the fluid-fluid interface is almost zero and the maximum value of $v_{x,2}(y, z)$ at a given *z* plane is strongly controlled by *β*. Accordingly, *β* is found by fixing μ_1 / μ_2 at 1000 or greater and fitting the velocity profile in the protein-lean phase, $v_{x,2}(y, z)$ to *β*. With this value of *β*, the ratio μ_1 / μ_2 is used to fit the velocity profile in the protein-rich phase, $v_{x,1}(y, z)$. The velocity profile that is fit in the protein-lean phase is generated by transforming the velocity values into a black and white image, finding the

edge where the density of points transitions from very high to very low, and transforming this back into velocity values (Fig. S4a). The resulting fit of Eq. S3 and S4 to the velocity edge values is given in Fig. S4b.

Supplemental References

1 H. Zhang, S. Elbaum-Garfinkle, E. M. Langdon, N. Taylor, P. Occhipinti, A. A. Bridges, C. P. Brangwynne and A. S. Gladfelter, *Mol. Cell*, 2015, **60**, 220–230.

2 S. Elbaum-Garfinkle, Y. Kim, K. Szczepaniak, C. C.-H. Chen, C. R. Eckmann, S. Myong and C. P. Brangwynne, *Proc. Natl. Acad. Sci. U. S. A.*, 2015, **112**, 7189–7194.

3 M. Feric and C. P. Brangwynne, *Nat. Cell Biol.*, 2013, **15**, 1253–1259.

Fig. S1: Device designs used for (a) microrheology only and (b) two-phase flow and microrheology experiments. Several pillars are designed in both devices to assist in droplet coalescence.

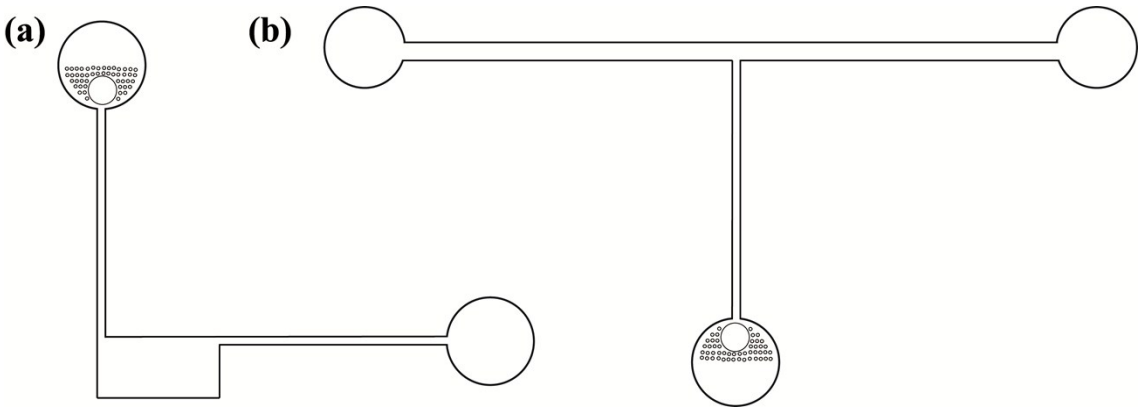

Fig. S2: Droplet phase (green) achieved after droplets settle onto coverslip with beads (red) rarely incorporated within them.

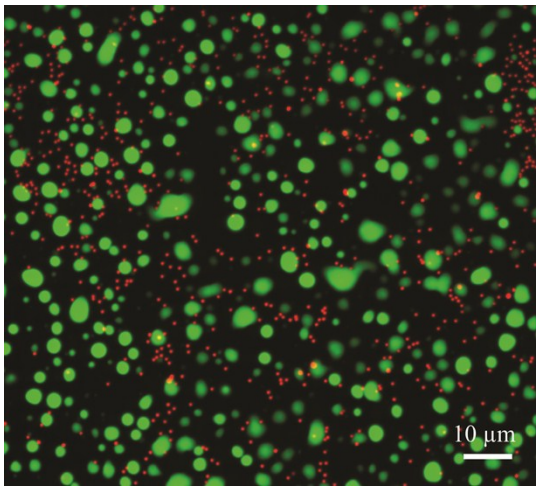

Fig. S3: Streaks (white) formed by beads in the protein-lean phase with overlaid centroids (yellow) corresponding to each streak.

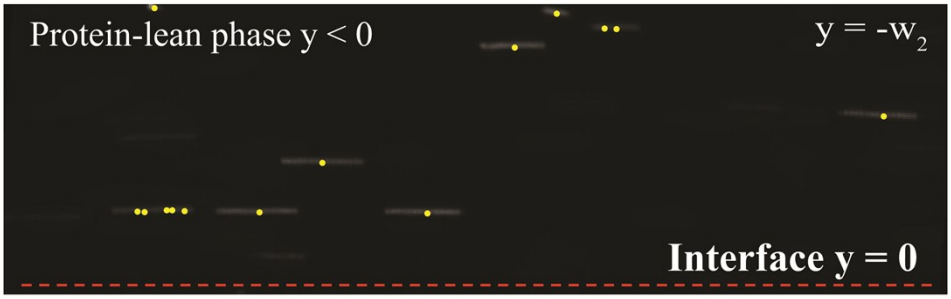

Fig. S4: (a) Measured velocity profiles in the protein-lean phase (filled black circles) with overlaid edge velocity profile (blue solid line) and (b) comparison of fit (red solid line) to edge velocity profile (blue filled circles).